fused product presented clear distinct forest stands and hence interpretable density. IHS-fused product gave the next best result, followed by Brovey's product.

The decision to choose the most suitable technique is influenced by specified application and can be supported by statistical validations. The PCS method should not be applied when correlation is small and replacing bands is not advantageous, if spatial resolution differs by a factor greater than two.

It has been widely observed in earlier research that IHS has become a standard procedure in image analysis, since it provides colour enhancement of highly correlated data[13] and improvement of spatial resolution[14,15]. IHS method has been recommended for different spatial and spectral resolution data[2,16,17]. IHS has the most effective and controlled visual presentation of the data, since other techniques produce images which are difficult to interpret quantitatively and qualitatively, as the statistical properties have been manipulated and original integrity of data is lost[18].

According to the present study, IHS method of data fusion distorted the data most in terms of spectral characteristics, but was very good at preserving the spatial components of high-resolution data sets. Brovey's method highly distorted the spectral value, but PCS fusion method changed the spectral values to the least, comparatively.

Also the PCS method was found to be good for visual interpretation of data at high scales, giving a high-resolution image of clear spectral values, making feature identification very easy. At the scale of 1 : 12,500, PCS-fused image presented a very clearly demarcated forest canopy and was thus appropriate for forest density stratification.

1. Chavez, P. S. Jr., *Photogramm. Eng. Remote Sensing*, 1986, **52**, 1637–1646.
2. Chavez, P. S., Sides, S. C. and Anderson, J. A., *Photogramm. Eng. Remote Sensing*, 1991, **57**, 295–303.
3. Saraf, A. K., *Int. J. Remote Sensing*, 1999, **20**, 1929–1934.
4. Pohl, C., Geometric Aspects of Multisensor Image Fusion for Topographic Map Updating in the Humid Tropics, ITC Publication, Enschede, The Netherlands, 1996, No. 39.
5. Koleijka, J. and Graf, H., *ZPF-Z.. Photogramm. Fernerkund.*, 1992, **2**, 49–59.
6. Schiewe, J., An Advanced Technique for Pixel-based Multi-Sensor Data Integration, Institute for Environmental Sciences, Vechta, Germany, 1999.
7. Loercher, G. and Wever, T., Proceedings of First International Airborne Remote Sensing Conf. and Exhibition, France, 1994, III-471–III-478.
8. Chiuderi, A. and Fini, S., Proceedings of 4th Workshop on Time-varying Image Processing and Moving Object Recognition, Florence, Italy, 10–11 June 1993.
9. Quattrochi, D. A. and Goodchild, M. F., *Scale in Remote Sensing and GIS*, Lewis Publishers, Florida, 1997.
10. Stoms, D., *Prof. Geogr.*, 1994, **46**, 346–358.
11. Turner, M. G., O'Neill, R. V., Gardner, R. H. and Milne, B. T., *Landscape Ecol.*, 1989, **3**, 153–162.
12. Steinnocher, K., *IEEE Proc.*, 1997.
13. Gillespie, A. R., Kahle, A. B. and Walker, R. E., *Remote Sensing Environ.*, 1986, **20**, 209–235.
14. Carper, W. J., Lillesand, T. M. and Kiefer, R. W., *Photogramm. Eng. Remote Sensing*, 1990, **56**, 459–467.
15. Welch, R. and Ehlers, M., *Photogramm. Eng. Remote Sensing*, 1987, **53**, 301–303.
16. Keys, L. D., Schmidt, N. J. and Phillips, B. E., *Technical Papers*, ACSM–ASPES Annual Convention, Image Processing and RS, 1990, vol. 4, pp. 238–249.
17. Franklin, S. E. and Blodgett, C. F., *Comp. Geosci.*, 1993, **19**, 577–583.
18. Harris, J. R., Murray, R. and Hirose, T., *Photogramm. Eng. Remote Sensing*, 1990, **56**, 1631–1641.

ACKNOWLEDGEMENTS. We thank the Director, NRSA for providing necessary facilities for this study.

Received 11 June 2001; revised accepted 16 August 2001

Possible relationship between temporal electrical resistivity variation and occurrence of the earthquake of 30 September 1993 in Latur region, Maharashtra, India

A. B. Narayanpethkar*, A. Vasanthi and K. Mallick**,†**

*Department of Geology, Shivaji University, PG Centre, Solapur 413 002, India
**National Geophysical Research Institute, Hyderabad 500 007, India

A lack of precise understanding of the complex earthquake processes has come in the way of earthquake prediction. It is well established that the hypocentral region of an earthquake undergoes structural and geological changes prior to its occurrence, leading to variation in physical properties of the rocks. In the present paper, the electrical resistivity measurements in and around Latur, Maharashtra, India from 1984 to the present time bring out an interesting correlation between earthquake occurrences and resistivity values. In intraplate stable continental regions like Latur where the possible location is broadly known, the temporal variations of electrical resistivity may zero down the period of occurrence of high magnitude earthquakes to a couple of months.

THE earthquake precursors and earthquake prediction are the burning issues among the earth scientists and engineers. Referring to a large number of important studies, Geller[1] has reviewed the investigations carried out in this

For correspondence. (e-mail: postmast@csngri.ren.nic.in)

direction over the past 120 years. Recently, Martin[2] conducted a Nature-online debate on earthquake prediction. As it appears from all these important studies, scientists are passing through ups and downs in the prediction strategies. Against this confusing backdrop, we report an interesting study on an intraplate earthquake in Latur region of Maharashtra, India and its correlation with the temporal variation in electrical resistivity.

The strong earthquake of magnitude 6.3 in the early hours of 30 September 1993 at Killari in Latur district (Figure 1), has left a trail of human misery and at the same time a storehouse of scientific queries. This region has experienced minor tremors in 1962, 1967, 1983 and 1984. The residents of this region have reported the occurrence of subterranean sounds[3] from time to time, for a very long time. Prior to the 1993 tremor, there were frequent shakings between 2 August 1992 and March 1993. During this period, the tremor on 18 October 1992 with magnitude 4 was the strongest. In the months of October and November 1992 alone, the seismological observatory at the National Geophysical Research Institute (NGRI), Hyderabad has recorded as many as nine tremors. The electrical resistivity in Ujjaini, about 25 km west of the epicentre of the Killari earthquake, recorded a sharp decay beginning from October 1992. Prior to these recent indications, scientists at NGRI have prepared isoseismal map[4], seismic zoning map[5] and maximum earthquake magnitude and peak horizontal ground acceleration maps[6] of India. All these features do indicate Latur region to be earthquake-prone. However, the 30 September 1993 earthquake with a high magnitude of 6.3, is a rare stable continental region (SCR) event, comparable in the twentieth century only to three events: Tenant Creek (Australia) earthquakes of 22 January 1988 with magnitudes 6.3, 6.4 and 6.7 within a span of 12 h and Ungava (Canada) earthquake of 25 December 1989 with magnitude 6.3 and Koyna earthquake of 10 December 1967 with a magnitude of 6.3 in India. Such intraplate events are not unusual though earthquake occurrences are, however, not so frequent as one finds them on the plate margins.

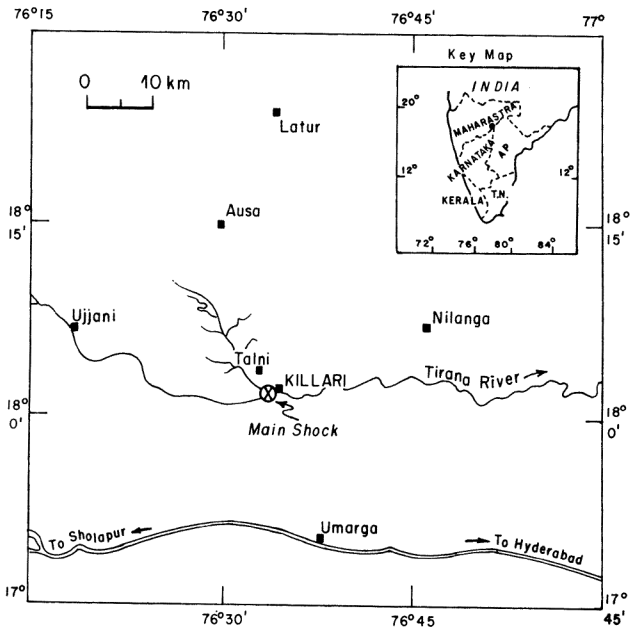

Figure 1. Location map of Killari earthquake of 30 September 1993 in Latur region, Maharashtra, India.

The fault plane solutions of the earthquakes occurring in the present collision zones and in plate margins are easily understood in terms of the geodynamic models. As regards the intraplate earthquakes at Koyna and Latur, the fault plane solutions cannot easily be correlated to any tectonic features. The reasons could be that there are no perceptible geologic processes active in this region at the present time and any previous plate tectonics, if at all remnant in this region, cannot easily be recognized.

In the present contribution, we have considered three aspects: possible correlation between (i) temporal variation in electrical resistivity and occurrence of earthquakes, (ii) isoseismicity and electrical resistivity distribution, and (iii) isoseismicity and lineament density.

Immediately after the earthquake, many national and international organizations carried out a variety of investigations, an important one being the recording of aftershocks by establishing many seismic stations. Details of all these studies are reported in a Special Publication of the Geological Survey of India[7]. In particular, Appa Rao *et al.*[8] have described post-earthquake variations in gravity and magnetic fields, and electrical resistivity values along a few profiles in Killari region. They found the low resistive top soil cover to extend up to a depth of about 15 m, and thicker the soil cover more is the damage. They attempted precursor studies to predict aftershocks.

Prior to the occurrence of earthquakes there are marked changes in the physical property of the earth material. Bolt[9] has postulated five stages of changes in physical properties: (i) Strain build-up (resistivity does not change), (ii) dilatancy and crack development (resistivity starts falling), (iii) influx of water and unstable deformation of fault zone (resistivity continues to fall), (iv) earthquake (resistivity value is lowest) and (v) drop in stress and aftershocks (sharp recovery in resistivity). Similarly, the Chinese group[10] classified the resistivity anomaly into three phases: (1) beginning stage (resistivity begins to drop), (2) lasting stage (stable drop in resistivity) and (3) accelerating stage (resistivity drops drastically). The third stage starts two to three months before the earthquake. The first and second stages may be recorded at epicentral distances of 100 to 200 km, whereas the imminent sudden drop in accelerating stage may be recorded at far-off locations. For instance, the sudden resistivity drop in case of Tangshan earthquake ($M = 7.8$; 28 July 1976) was observed at a distance of

550 km. It may be noted here that the great Shillong earthquake ($M = 8.7$, 6 December 1897) had induced liquefaction in regions as far as Motihari and Madhubani in Bihar!

In light of the above field simulation and continuous resistivity measurements in China and Central Asia, we tried to understand the resistivity changes recorded at Ujjaini in Latur region.

Starting from 1983, electrical resistivity soundings with Wenner configuration were taken every year, mostly during winter and summer seasons, for groundwater exploration over an area of about 1000 sq km in and around the epicentre of the Killari earthquake of 30 September 1993. These measurements have enabled us to study the changes in the electrical resistivity over a period of nearly 15 years. Systematic resistivity measurements in an earthquake-prone area spreading over 15 years, provide rare as well as useful data.

Figure 2 shows the changes in resistivity values for different electrode separations, $a = 25$, 50, 75 and 100 m in Ujjaini, about 25 km west of the epicentre of the earthquake from the middle of 1984 to May 2000. Up to 1995, each point represents an average of stacked resistivity values of about 10 soundings, whereas after 1995 each point is a stacked value of three to four resistivity soundings. Along with the resistivity values, the occurrence of some tremors of magnitude three or more are also shown.

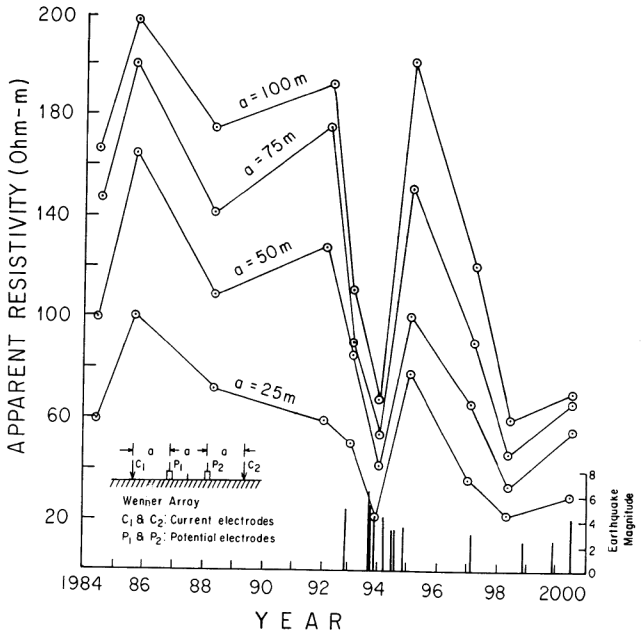

Figure 2. Variation of electrical resistivity values for different Wenner electrode spacings in Ujjaini, about 25 km WNW of the epicentre of Killari earthquake. Fall in the resistivity values from the beginning of 1993 is remarkable. Lowest resistivity values for all electrode separations show strong correspondence with occurrence of the tremor.

A detailed analysis of Figure 2 is given later in this communication.

The earthquake mechanism, in essence, forms a cycle of progressive accumulation of strain over a long period of time and its sudden release. This process in certain tectonic regions is repetitive, i.e. the earthquakes do reoccur and seismologists are yet to evolve perfect techniques to estimate return times. The onset of an earthquake deforms the focal or hypocentral region. The innermost focal zone virtually turns into a void, surrounded by an anelastic crushed zone. The anelastic crushed zone gradually grades into an elastic medium. Tectonic forces often produce the strain along the existing faults. Several months or even years, in case of large earthquakes, prior to their occurrences, deformations, fractures, crevices and cracks develop in rocks, resulting in increase in porosity and permeability.

The strain, cracks and crevices in rocks find expression in a variety of changes, local as well as regional, such as vertical displacement, increased emanation of radon gas and tilt near the active fault. The length of the fault (L) depends on the magnitude (M) of an earthquake[11], and is statistically expressed by

$$M = 3.3 + 2.1 \log L. \quad (1)$$

The extent of the affected region is two to three times the length of the fault. In the Latur earthquake ($M = 6.3$), for instance, the length of the fault or the dislocation is about 30 km and the affected region is about 60 to 90 km around the epicentre at Killari. For a large earthquake like Shillong ($M = 8.7$) of 1897, the fault or dislocation length was about 370 km and the affected region was between 750 and 1000 km around the epicentre.

The deformation due to tectonic forces is one side of the story. There is another equally important factor that controls the earthquake mechanism, namely the presence of water – interstitial as well as in cracks and crevices[9]. Increase in pore pressure leads to the reduction in seismic wave velocity (dilatancy hypothesis, once considered to be a successful tool to forecast earthquakes); reduction in shearing strength of rocks; filling of microcracks and fault planes that provide required lubrication for release of strain; developing shear slip to produce slickensides; production of hydrous rocks such as serpentinite at depths[9,12] and zeolites, specially in basaltic terrain at shallower horizon, evidenced by the presence of conductive zone in earthquake-prone regions; reduction in magnetic field and electrical resistivity; changes in groundwater table and water quality. All these features are not necessarily associated with each and every earthquake. In the Latur earthquake, for instance, the following features were reported:

(i) Fractured and crushed rocks like breccia and clay near Rajegaon along Tirna river indicated hydrological conditions typical for an earthquake to facilitate shear slip,

evident by the presence of slickensides on the fault plane of a reverse fault[13].

(ii) Direct drilling[14] that encountered the basement granite at a depth of 338 m confirmed the reverse fault as well as the fractured and crushed basaltic rocks. This is the reason of high yield of wells in the earthquake-affected region.

(iii) Presence of a conducting zone, may be due to serpentinization, at a depth of about 7 km in Killari region was established by magnetotelluric measurements[15]. Serpentinization, besides producing a conductive zone, lowers seismic velocity and density of rocks as well. The presence of a low-density zone surrounded by high-density layers sets in inequilibrium; a crude comparison with an air-filled football inside water! It creates locally an inward compression from all sides, a situation nearly similar to a marine source like vaporchoc, to create an explosion leading to dislocation and faulting in the rock strata.

(iv) The groundwater table during November 1992 in Latur region was 16.75 m below ground level[16], whereas during 1986–1987 the same varied between 6 and 14 m below ground level[17]. This is expected from the findings of Jain *et al.*[16] that there was a decrease in groundwater table by 20 to 30 cm/year over the past 7 to 15 years, thereby lowering the groundwater table by about 4 to 5 m.

(v) During and immediately after the earthquake, the groundwater table had increased by 2–3 m and yet at some other place the dug wells went dry. The opening of cracks and crevices created more porosity and permeability. The groundwater may flow from one place to another, thereby decreasing the groundwater table in the former horizon and increasing the same in the latter.

(vi) The temperature, pH and TDS of groundwater did not change compared to the previous years, 1986–1987. Near the epicentral area high silica, magnesium, chlorine and potassium content were reported by Karve[18] indicating possible association of geothermal activity with the Latur earthquake.

(vii) More damage was reported from regions with thick soil cover, loose sediments and weathered material, often on both sides of the streams.

The main contention of the present paper is an explanation for the above phenomenon. This feature would be better understood by describing similar studies, first a field simulation and then continuous measurements undertaken in China and Russia in an attempt to predict the impending earthquakes.

A field experiment was conducted on the partially saturated wall of an underground tunnel in a mine to establish a relationship between loading and unloading within elastic limits on one hand, and the corresponding changes in resistivity on the other. Figure 3 shows the results of the experiment. During the compression, the resistivity decreases progressively and increases very sharply at the point of unloading.

The same group of investigators[11] have studied the resistivity changes in case of five strong earthquakes in China, Luhao ($M = 7.9$) on 6 February 1973, Zhaotong ($M = 7.1$) on 11 May 1974, Longling ($M = 7.6$) on 29 May 1976, Tangshan ($M = 7.8$) on 28 July 1976 and Sangpan ($M = 7.2$) on 16 August 1976.

The resistivity values at Wadu station, 100 km away from the epicentre of the Sangpan earthquake, shown in Figure 4, started falling from the beginning of 1975, showed a rise towards the end of 1975, started falling again and coinciding with the lowest resistivity value, the violent earthquake took place on 16 August 1976. Corresponding with the first low during mid-1975, there were no earthquakes. Since the resistivity changes are affected as far as 300 to 400 km from the earthquakes, some of the lows riding the general trend of resistivity decrease may correspond to distant tremors. In case of the Tangshan earthquake ($M = 7.8$) on 28 July 1976, resistivity minimum at the time of its occurrence was recorded at a station 550 km away!

In yet another example, in case of the Luhao earthquake ($M = 7.9$) that occurred on 6 February 1973, resistivity measurements were made at Garze, 45 km away from the

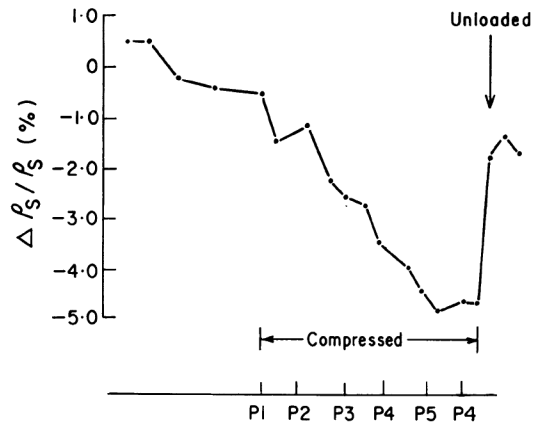

Figure 3. Experiment conducted by Lanzhou Earthquake Research Institute, China to study the variations in electrical resistivity during the process of loading and unloading.

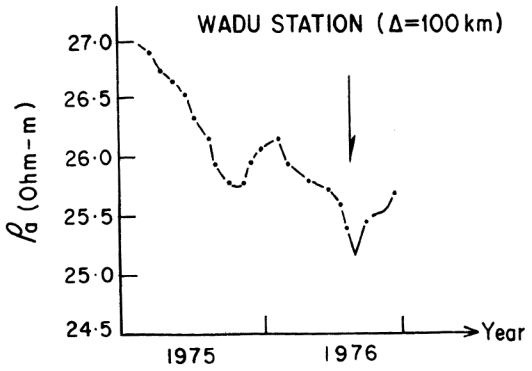

Figure 4. Changes in apparent resistivity before the Sangpan earthquake[11] ($M = 7.2$).

epicentre during 1972–1973. During February and October 1972 there were small lows in resistivity variations, which did not correspond to any tremors.

We take the final example from Central Asia, described by Mogi[19]. Figure 5 shows the temporal variation in apparent resistivity at Garm continuously during 1967-1968, partly in 1969 and 1970, and again continuously during 1971–1973 along with the occurrence of earthquakes. Earthquake occurrences did correspond to the low resistivity values, with one exception during mid-1967. As we have stated earlier, this low may correspond to some distant tremor!

Taking clues from these important observations, we turn our attention to understand the patterns of resistivity changes in Latur region. One of the most interesting features has been the variation of electrical resistivity (shown in Figure 2) over a period of 16 years, spanning between 1984 and 2000. The measurements made in and around Ujjaini, about 25 km from the epicentre, perhaps only one such example in India, showed a possible correspondence between decrease in resistivity values and the onset of earthquake tremors during 1983, 1993–1994 and 1997–1999. The decrease in resistivity during 1993, and the third quarter in particular, was spectacular.

It may be noted that the resistivity changes in Figure 4 at Wadu station in case of Sangpan earthquake, has a very narrow range, 25–27 ohm-m. In contrast, Figure 2 showed a range of 64–186 ohm-m in resistivity values for electrode separation 100 m at a distance of about 25 km from the main shock at Killari. Therefore, the post-1995 measurements averaged over four to five soundings, are significant.

Figure 2 shows the following features:

(i) The resistivity low during 1983 for all electrode separations has recovered from the beginning of 1984. The occurrences of a number of tremors during 1982–1983 (ref. 3) explain the fall and rise in resistivity values.
(ii) There is a broad low in resistivity values during 1988. *In situ* stress measurements by Gowd *et al.*[20] near Latur showed the maximum horizontal compressive stress to have an orientation of N35°E. It is possible that this compressional stress is also responsible for lowering the resistivity in Ujjaini area. The absence of a sharp recovery in resistivity value, in particular for electrode separation, a = 25 m, indicates that there is no sudden unloading of stress. This feature may suggest that the resistivity decrease during this period is not controlled by earth tremors. The ramp-like increase in resistivity values for other electrode separations, a = 50, 75 and 100 m, may be due to unloading of stress at some remote places. (We are not certain whether the Bihar earthquake of 20 August 1988 with a magnitude of 6.4 could cause a recovery in resistivity values[11]!)
(iii) The fall in resistivity values beginning from 1992 up to the last quarter of 1993 is spectacular. The major event of 30 September 1993 (M = 6.3) shows significant agreement with the resistivity low.
(iv) In Bolt's[9] postulated model, this corresponds to stage IV (occurrence of earthquake), followed by stage V that showed recovery of resistivity values and aftershocks. The results of the simulated experiment, shown in Figure 3, admirably agree with these observations.
(v) In contrast, the fall in resistivity after 1996 shows less steepness compared to the post-1992 gradient, and a moderate tremor (M = 3) is recorded in the first quarter of 1997. Instead of recovery, the resistivity continues to fall till the first quarter of 1998, after which there is a rise. The measurements in May 2000 recorded relatively sharp rise for a = 50 and 75 m, a tremor (M = 4) took place in Killari in the following month, June 2000. Apparently, broader low is associated with tremor of low magnitude.

More than the decrease in resistivity values, it appears as if the steepness in resistivity gradient and the magnitude of the earthquake have direct correspondence. The electrical resistivity in other locations like Ausa showed similar trends, specially during 1992–1994. In view of this, the resistivity anomaly in Figure 2 is not a local phenomenon, but most likely reflects the coseismic ground condition in and around Killari region within a radius of 60 to 90 km, according to the relation in eq. (1).

For the earthquakes like Lahuo, Zhaotong, Longling, Tangshan and Sangpan in China, resistivity measurements were made at stations as far as 200 to 300 km from the epicentre. However, we believe that if 15 to 20 stations in the proximity of Killari within a radius of 50 km are selected and monthly measurements of electrical resistivity are taken, the patterns in the changes of resistivity values would enable geologists to predict the onset of major events (magnitudes exceeding 5 and above) two to three months in advance.

A precaution is required. The interfering effects by the distant earthquakes need to be resolved prior to establishing the local anomaly in resistivity values for correct prediction. The lows in resistivity values observed in

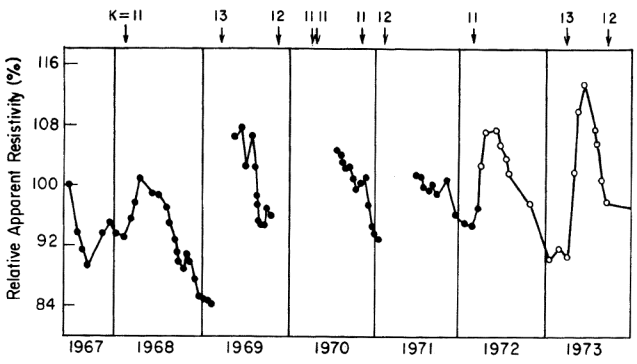

Figure 5. Changes in apparent resistivity observed at Garm, Central Asia for a number of earthquakes. Segments of the curve with filled circles are by Barsukov and Sorokin[23] and the segment with open circles, by Sadovsky[24]. Earthquake occurrences are indicated by arrows with Russian magnitude, K.

Figure 3 in case of Sangpan earthquake during 1975, might reflect possible interference by distant earthquakes.

The degree and extent of damages due to earthquakes are presented by isoseismal maps. The Geological Survey of India[7] (GSI) and NGRI[4] have independently prepared the isoseismal maps of the Killari earthquake. The regions of damage are found to have relatively low resistivity.

In a region lying between lat. 17°45′ and 18°20′N and long. 76°00′ and 76°45′E, a large number of resistivity soundings with Wenner array were taken during 1992–1993. Stacking a number of resistivity values for different electrode spacings, a = 10, 25, 50, 75 and 100 m, resistivity contour maps have been prepared. The general patterns of the resistivity distribution for all the five electrode separations and the degree of damage represented by the isoseismal map have good agreement. We illustrate the resistivity contour map for two out of the five electrode spacings, a = 10 and 100 m, along with isoseismal map prepared by GSI[7] superimposed on it. While the resistivity contours for a = 10 m in Figure 6 represent the shallower effects, those for a = 100 m in Figure 7 indicate ground conditions up to a depth of about 100 m. It is interesting to note in Figure 6 that (i) the low resistivity contour (10 ohm-m) passes near Killari and Sastur, the zone that had the epicentre and suffered maximum damage, (ii) the isoseismal lines with intensity VIII and IX enclose Killari, Sastur and Lohar, and (iii) in a qualitative way the isoseismal and the resistivity contours show similar patterns on the south-west and southern parts.

For other electrode spacings, a = 25, 50 and 75 m, the epicentral region does show lower resistivity values. With the gradual increase in electrode spacings, however, the depth of investigations as well as the lateral spread of the resistivity contours increases, thereby bringing in a better correspondence between the isoseismal lines of lower intensity and the resistivity contours. The resistivity and isoseismal contours show elliptical patterns directed towards the south-west.

The presence of soil and unconsolidated rocks in and around the epicentre often enhances the degree of damage, due to a wave-guide effect. The seismic waves that enter into such a zone reflect back and forth and the wave amplitudes, keep increasing instead of decreasing and often match the natural frequency of different structures like buildings, overhead tanks, dams, etc. This, in turn, creates a resonant situation and causes large-scale damages. This might have happened in the Killari region. Numerous electrical soundings indicate the thickness of the soil, weathered and unconsolidated rocks to be of the order of 30 to 50 m. Appa Rao *et al.*[8] also reported similar values along a N-S profile. In view of this, we illustrate the resistivity contour map for electrode spacing a = 100 m, along with the isoseismal map.

The resistivity contours corresponding to the electrode spacing a = 100 m resolved two low-resistivity pockets in Figure 7 that align convex towards the SW direction lying on the isoseismal contour with intensity VII and, therefore, appear to migrate in the SW direction.

For both the electrode separations, a = 10 and 100 m, the general pattern of an elliptical wedge of low resistivity

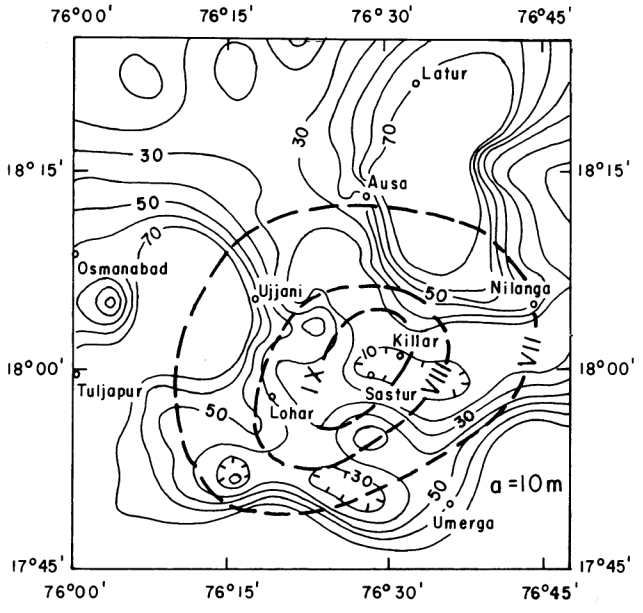

Figure 6. Electrical resistivity contours for Wenner electrode separation of 10 m in and around Killari region. Epicentral region shows the lowest resistivity of 10 ohm-m. Isoseismal contours show a good correspondence, particularly at the central and south-west region. Contour interval: 10 ohm-m.

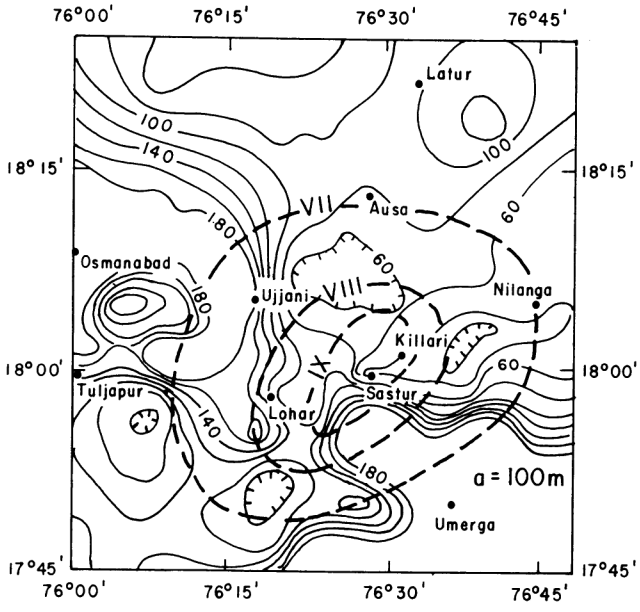

Figure 7. Electrical resistivity contours for Wenner electrode separation of 100 m for the same region as in Figure 3. The contour closure of 20 ohm-m has a shift towards east of Killari. On south-west corner, there are three resistivity contour closures that are convex towards south-west, parallel to the isoseismal contour. Contour interval: 20 ohm-m.

convex towards south-west remained prominent and showed good correspondence with the shape of the isoseismals. While the resistivity values for the electrode spacing $a = 10$ m correspond to the top soil, those for $a = 100$ m represent the underlying weathered rocks. Both the top soil and the weathered basalts show low-resistivity. Seismically, this is also a low velocity zone. It forms a wave guide, a potential zone of hazard.

The correlation between the contour patterns of the low resistivity and isoseismals, as observed in and around the Killari earthquake region, may provide a means to map in advance, the zones prone to earthquake damage.

The lineaments in and around Killari have been identified from satellite images on a 1 : 2,50,000 scale by Chetty and Rao[21]. The lineaments have two prominent trends, one along NW-SE and the other along NE-SW. There are also a few N-S and ENE-WSW trending lineaments. Based on the field observations and ground truths, the NE-SW and ENE-WSW trending sets of lineaments are believed to be younger[21]. Geomorphologically, the lineaments often give rise to a network of straight drainage, facilitate weathering and produce high-yielding wells and tectonically represent zones of fractures and faults. Rose diagrams and the density of intersection points of two sets of lineaments are often used to qualitatively interpret the lineaments.

In the present communication, we offer another approach to quantify the lineament density. The region shown in Figure 8, for which the lineaments were identified by Chetty and Rao[21], is divided into 7 × 7 blocks. The lineament lengths in each block, separately for NE-SW and NW-SE trending sets, were measured and added, plotted at the centre of each block and then contoured. The unit of the lineament density contour is the kilometre.

Figure 8 shows the lineament density contours for the NE-SW trending set of lineaments. The main features are:

(1) The zone showing highest lineament density contour of 90 km lies south-west of Killari.
(2) The lineament density contour showing 50 km enclosing Killari and Matola shows good correspondence with the isoseismal contours.
(3) East of Ausa and north of Nilanga, there are two lineament density contour closures. These two regions were heavily affected by the earthquake.
(4) The outer 40 km lineament density contour, east of Nilanga, north of Umarga, encloses a larger region that has a north-west bulge. The isoseismals too are more convex towards the north-west direction.

According to the tectonic set-up, the south-western side has thrusted over the north-western part across a reverse fault and runs south of Killari and strikes NW-SE[22]. The highest lineament density (90 km) south-west of Killari corresponds to the up-thrusted hanging wall and the 50 km contour appeared to be caused by compression from the south-west direction. The footwall is sheared to produce a region of high lineament density, east of Ausa and north of Nilanga.

The NW-SE trending lineaments, on the other hand, do not show any agreement with the isoseismal contours and appear to have less role in the occurrence of the Killari earthquake, perhaps because this set of lineaments is older and is remnant of an earlier tectonics. The younger lineaments with NE-SW trend, on the other hand, primarily control the occurrence of the earthquake and the propagation of the seismic energy, causing large-scale damages. The density contour of the set of NE-SW trending lineaments and the resistivity contour with varying electrode spacings show close relationship with each other in the south-western parts of the present study area in particular. The lineament contours and resistivity contours in this region show a good correspondence with the isoseismals.

To conclude, the present study based on resistivity changes from 1984 to 2000 and analysis of lineament density has brought out several interesting features for the earthquake of 30 September 1993 in Latur region, Maharashtra. It is observed that the occurrence of the earth tremors has good correspondence with lowering of the electrical resistivity. In fact, the event of 30 September 1993 had caused a three-fold decrease in the background resistivity value of about 200 ohm-m to less than 60 ohm-m for electrode separations, $a = 75$ and 100 m, over a short period of about nine months. This observation suggests that in case of intraplate earthquakes in regions like Latur where the location is more or less known, it may be possible to predict the time of occurrence at least three to four months in advance, if resistivity measurements are taken on a monthly basis and changes in resistivity values are regularly monitored.

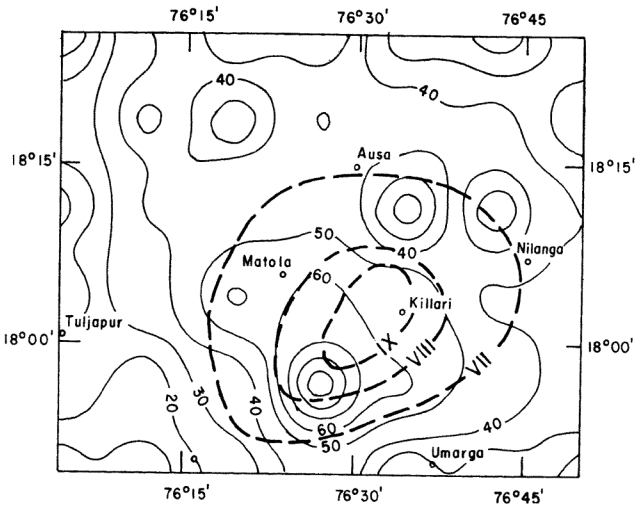

Figure 8. NE-SW trending lineament density contour and isoseismal contour maps in and around Killari region. The lineament density contours have strike similar to that of the isoseismal contours. Contour interval: 10 km.

Hazard assessment is another important issue in earthquake-prone areas. The meizoseismal and isoseismal maps are prepared after the earthquake has occurred and the damages are assessed. However, it is observed in Latur region that zones of low resistivity are more prone to damages. Keeping this aspect in view, it is possible to prepare the resistivity contour maps and update them from time to time in order to identify the zones likely to be damaged.

The network of lineaments and their density contours, as observed in the Latur region, may act as a forerunner for hazards. The NE-SW trending lineament density map shows strong correspondence with the isoseismal contours. In the light of this, if the lineaments from the satellite imageries are interpreted annually and the changes in lineament density are monitored, one can succeed in identifying the zones of possible hazards.

To conclude, the temporal resistiviy variations are of use in earthquake-prone areas for possible prediction and hazard assessment.

1. Geller, R. J., *Geophys. J. Int.*, 1997, **131**, 425–450.
2. Martin Ian, Debate on Earthquake Prediction, *Nature – Online*, http://helix.nature.com/debates/earthquake, 1999.
3. Asolkar, M. R., Report, Directorate of Geology and Mining, Govt. of Maharashtra, Aurangabad, 1983, pp. 1–37.
4. Kaila, K. L. and Sarkar, D., *Geophys. Res. Bull.*, 1978, **16**, 233–267.
5. Kaila, K. L. and Madhava Rao, N., *Geophys. Res. Bull.*, 1979, **17**, 293–301.
6. Kaila, K. L. and Prasad Rao, P., Proceedings of the Fourth International Conference on Seismic Zonation, 26–29 August, Stanford University, California, USA, 1991.
7. *Geol. Surv. India, Spec. Publ.*, No. 27, 1995.
8. Appa Rao, M., Sastry, C. B. K., Ananda Reddy, R., Somayajulu, P. S. and Srinivas, S., *Geol. Surv. India, Spec. Publ.*, No. 27, 1995.
9. Bolt, Bruce, A., *Earthquakes*, W. H. Freeman, New York, 1993, vol. XIII, p. 331.
10. Zongjin, M., Zhengxiang, F., Yingzhen, Z., Chengmin, W., Guomin, Z. and Defu, L., *Earthquake Prediction (Nine Major Earthquakes in China)*, Springer Verlag, 1990, p. 332.
11. Jiadong Qian, Xai Gui, Huaizhou Ma, Xikang Ma, Huapina Guang and Qingming Zhao, Proc. of Int. Symp. on Earthquake Prediction, Terra Scientific Publishing, UNESCO, Paris, 1984, pp. 145–155.
12. Rao, V. K. and Prasad, S. N., *Earth Planet. Sci. Lett.*, 2001, **190**, 79–91.
13. Gupta, H. K., Rao, R. U. M., Sreenivasan, R., Rao, G. V. and Reddy, G. K., *Geophys. Res. Lett.*, 1999, **26**, 1985–1988.
14. Gupta, H. K. and Dwivedy, K. K., *J. Geol. Soc. India*, 1996, **47**, 129–131.
15. Sarma, S. V. S. *et al.*, *Mem. Geol. Soc. India*, 1994, 35, 101–118.
16. Jain, S. K., Marwaha, S., Agashe, R. M. and Mehta, M., *Geol. Surv. India, Spec. Publ.*, 1995, 27, 243–250.
17. Singh, R. P., Report, Central Groundwater Board, 1987.
18. Karve, A. K., *Geol. Surv. India, Spec. Publ.*, 1995, 27, 235–242.
19. Mogi, K., in *Earthquake Prediction*, Academic Press, New York, 1995, p. 355.
20. Gowd, T. N., Sri Rama Rao, S. V., Chary, K. B. and Rummel, F., *Proc. Indian Acad. Sci. (Earth Planet. Sci.)*, 1986, **95**, 311–319.
21. Chetty, T. R. K. and Rao, M. N., *Mem. Geol. Soc. India*, 1994, **35**, 65–73.
22. Gupta, H. K., *Curr. Sci.*, 1992, **62**, 257–263.
23. Barsukov, O. M. and Sorokin, O. N., *Acad. Sci. USSR, Phys. Solid Earth* (Engl. Trans.), 1973, **8**, 685–687.
24. Sadovsky, M. A., (ed.) *Inst. Zemli. Akad. Nauk. USSR* (Japanese edn).

ACKNOWLEDGEMENTS. We thank Dr H. K. Gupta, former Director, NGRI and presently Secretary, Department of Ocean Development, Govt. of India, for his keen interest and Dr S. M. Naqvi, Acting Director for his permission to publish the paper. We thank Mr G. Ramakrishna Rao for help in preparing the manuscript and Mr Sham Vaidya in drafting the figures. We also thank the reviewer for very constructive comments to improve the paper.

Received 5 February 2001; revised accepted 19 June 2001

18 Ka BP records of climatic changes, Bay of Bengal: Isotopic and sedimentological evidences

Onkar S. Chauhan* and J. Suneethi

National Institute of Oceanography, Dona Paula, Goa 403 004, India

Based upon the oxygen isotopic records of *Globigerinoide sacculifer*, the clay mineral assemblages and aridity indicator chlorite/illite (C/I) ratio, the palaeoclimatic changes during the past 18 Ka BP have been archived. The results show intense arid climate between 18 and 15 ^{14}C Ka BP, a variable climate between 15 and 13 Ka BP, and again an arid climate at 12.5 Ka BP. The negative $\delta^{18}O$, reduced C/I and higher smectite document a humid phase culminating at 12 Ka BP. Arid climate phases are also identified at 10.3 and 11.5 Ka BP. The later event matches well with that of the 'Younger Dryas' event of world climate models. The beginning of the Holocene is marked by lighter $\delta^{18}O$ values (at around 9.5 Ka BP), which has been interpreted as onset of a humid phase and high freshwater influx into the bay, correlating with the world climatic event 'mwp IB'. We also identify two more arid events at ~ 4800 and 2300–2200 yr, hitherto unreported from the Bay of Bengal.

Monsoon variability in the Indian subcontinent is regulated by coupled heating–cooling between the Himalayas and the southern Indian Ocean[1–3]. There are two monsoon seasons, i.e. the NE and the SW prevalent during boreal winter and summer respectively. The SW monsoon accounts for over 80% of rainfall in the Indian subcontinent.

*For correspondence. (e-mail: onkar@darya.nio.org)